SPE-168967-MS

Simulation of Coupled Hydraulic Fracturing Propagation and Gas Well Performance in Shale Gas Reservoirs

Xu Wang, CNP CUSA Corporation; Philip Winterfeld, Colorado School of Mines; Xu Ma, Changqing Oilfield Company, Petrochina; Dengsheng Ye, Chuanqing Drilling Engineering Company Limited, CNPC; Jijun Miao and Yonghong Wang, CNP CUSA Corporation; Cong Wang and Yu-Shu Wu, Colorado School of Mines

This paper was prepared for presentation at the SPE Unconventional Resources Conference – USA held in The Woodlands, Texas, USA, 1-3 April 2014.

Abstract

Hydraulic fracturing combined with horizontal drilling has been the technology that makes it possible to economically produce natural gas from unconventional shale gas reservoirs. For best performance of fracturing stimulation, hydraulic fracturing designing parameters, such as different proppants, fracturing liquids, and injection rate and pressure, should be evaluated before the oeration in a particular reservoir system. Traditional evaluation and optimization approaches are usually based on the simulated fracture properties along, such as fracture areas. In our opinion, the better methodologyshould be also related to production data from the stimulated wells afterwards, because the enhanced production is the ultimate goal.

In this paper, we present a general fully-coupled numerical framework to simulate the hydraulic induced fracture propagation and post-fracture gas well performance. This three-dimensional, multi-phase simulator focuses on: (1) fracture width increase and fracture propagation that occurs as slurry is injected into the fracture, (2) erosion caused by fracture fluid and leakoff, (3) proppant subsidence and flowback, and (4) multi-phase fluid flow through various-scaled anisotropic natural and man-made fractures. Mathematical and numerical details on how to fully couple the fracture propagation part and the fluid flow part are discussed. Fracturing and production operation parameters, properties of the formation, and reservoir, fluid, and proppant properties are all taken into account in this model. The well may be horizontal, vertical, or deviated, as well as open-hole or cemented. This simulator is verified based on benchmarks the literature. We show its application by simulating the fracture network (hydraulic and natural fractures) propagation and production data history matching of field production data in China. We conduct a series of real-data modeling studies with different combinations of fracturing parameters and present the methodology to design fracturing operations with feedback of simulated production data. This unified model aids in the optimization of hydraulic fracturing design, operations, and production.

Introduction

A fully coupled numerical framework to simulate the hydraulically induced fracture propagation and post-fracture gas well performance is important for the optimization of hydraulic fracturing design and oil/gas production. Generally, several interconnected physical processes need to be considered: (1) fracture width increase and fracture propagation occurring as slurry is injected into the fracture, (2) erosion caused by fracturing fluid and leakoff, (3) proppant subsidence and flowback, and (4) multi-phase fluid flow through various-scaled anisotropic natural and man-made fractures. In this paper, we introduce the theory and methodology for simulating fracture propagation and multi-phase flow separately, and afterwards a numerical framework to couple them.

The primary objective of the multi-phase flow portion is to develop an efficient reservoir simulator for modeling multidimensional gas and water flow and production from unconventional tight sandstone or shale gas reservoirs. Specifically, it includes: (1) developing conceptual models and improved modeling approaches for integrating hydrological, mechanical, and physical processes in hydraulically fractured tight sand and shale gas reservoirs; and (2) incorporating conceptual models into a numerical modeling tool for assessment and management of gas production from tight sand gas reservoirs using hydraulically fractured wells. The lattrer part of the developed simulator is able to quantify model physical processes and predict long-term performance of tight gas reservoirs for optimum gas production from these unconventional resources.

The goal of the fracture propagation portion is to develop a three-dimensional, single-well simulation model for use in design and evaluation of hydraulic fracturing processes in tight gas and shale gas reservoirs. The single well may be horizontal, vertical, or deviated, and may also be open-hole or cemented. The reservoir portion of the model would be the standard reservoir flow formulation based on Darcy's law and conservation of mass. Such a model is characterized by rock porosity and permeability and fluid pressure and saturations. These rock properties will be spatially variable and fluid phases will be aqueous and gas.

Theory and Methdology

1) Fracture Mass and Flow Equations

We consider a fracture to be a thin, planar slit. The fracture width is in the y-direction and the fracture plane in the other two dimensions. Slurry, consisting of fluid and proppant components, flows through the fracture and the slurry components are conserved. The proppant conservation equation is:

$$\frac{\partial[\rho_p \vec{v}_p c_p w]}{\partial x} + \frac{\partial[\rho_p \vec{v}_p c_p w]}{\partial z} + \frac{\partial}{\partial t}\left[\rho_p c_p w\right] = 0 \quad (1)$$

and the fluid component conservation equation is:

$$\frac{\partial[\rho_f \vec{v}_{fl} x_f (1-\sum_p c_p) w]}{\partial x} + \frac{\partial[\rho_f \vec{v}_{fl} x_f (1-\sum_p c_p) w]}{\partial z} + \frac{\partial}{\partial t}\left[\rho_f x_f \left(1-\sum_p c_p\right) w\right] + \dot{q}_{leak} \rho_f x_f = 0 \quad (2)$$

where c_p is proppant volume fraction, x_f is fluid volume fraction relative to total fluid, ρ is density, $\vec{v}$ is velocity, w is fracture width, and $\dot{q}_{leak}$ is the fluid leakoff rate per unit area.

We assume fluid and proppant to be incompressible in the fracture. Then, densities in Equations 1 and 2 cancel. We sum those equations over proppant and fluid components, respectively, and add the two to obtain an overall slurry balance:

$$\frac{\partial[(\sum_p c_p \vec{v}_p + (1-\sum_p c_p)\vec{v}_f) w]}{\partial x} + \frac{\partial[(\sum_p c_p \vec{v}_p + (1-\sum_p c_p)\vec{v}_f) w]}{\partial z} + \frac{\partial}{\partial t}[w] + \dot{q}_{leak} = 0 \quad (3)$$

We equate the coefficient of w in the derivative terms to the slurry velocity:

$$\vec{v}_{sl} = \sum_p c_p \vec{v}_p + \left(1-\sum_p c_p\right)\vec{v}_{fl} \quad (4)$$

and assume slurry velocity is that for laminar flow through a slit of width w:

$$\vec{v}_{sl} = -\frac{w^2}{12\mu_{sl}} \nabla(P + \gamma z) \quad (5)$$

where P is fracture pressure, μ_{sl} is slurry viscosity, and γ is slurry gradient.

Slurry viscosity depends on proppant volume fraction as well as fluid component rheology.A number of expressions have appeared in the literature for the viscosity of suspensions containing solid particles (for example, Nicodemo et al., 1974) and we use the common exponential relation of the form:

$$\mu_{sl} = \mu_{fl}\left(1 - \frac{\sum_p c_p}{c_{max}}\right)^{-n} \quad (6)$$

where μ_{fl} is the fluid viscosity, c_{max} is the maximum proppant volume fraction at which slurry is essentially a solid porous medium, and n is an exponent typically between 1.0 and 2.5.

For z-direction flow, proppant particles settle because proppant is more dense than fluid; for x-direction flow, proppant velocity differs from slurry velocity due to inertial effects and the effect of slurry particles colliding with each other and the fracture wall. Friehauf (2009) presented expressions for these effects. The z-direction proppant, settling velocity has the form:

$$v_{stl,z} = v_{stokes} f(N_{re}) g(c_p) h(w) \quad (7)$$

where v_{stokes} is the Stoke's settling velocity, $f(N_{re})$ captures inertial effects, $g(c_p)$ captures the effect of interfering proppant particles, and $h(w)$ captures the effect of the fracture wall on proppant velocity. The z-direction proppant velocity component is the sum of the slurry and settling velocity components:

$$v_{p,z} = v_{sl,z} + v_{stl,z} \tag{8}$$

For x-direction flow, the fracture wall and other proppant particles both retard the proppant velocity:

$$v_{p,x} = k(c_p, w)v_{sl,x} \tag{9}$$

where $k(c_p, w)$ is a function quantifying these effects.

The pressure difference between the fracture and the permeable reservoir causes fluid to leak off into the formation. Fluid leakoff is accompanied by the buildup of a filter cake at the fracture wall, a growing invaded zone of fracture fluid in the formation starting at the fracture wall, and the compression of the formation fluid from this growing invaded zone. Each of these leakoff mechanisms has been described by a leakoff coefficient (Schechter, 1992) and these leakoff coefficients are combined into an overall leakoff coefficient, C_{tot}:

$$C_{tot} = \frac{-\frac{1}{C_c} + \sqrt{\frac{1}{C_c^2} + 4\left(\frac{1}{C_v^2} + \frac{1}{C_w^2}\right)}}{2\left(\frac{1}{C_v^2} + \frac{1}{C_w^2}\right)} \tag{10}$$

whereC_w, C_v, and C_c are leakoff coefficients for the filter cake, invaded zone, and compressible formation, respectively, with fluid leakoff rate given by:

$$\dot{q}_{leak} = \frac{2C_{tot}}{\sqrt{t-\tau}} \tag{11}$$

where τ is the leakoff start time.

2) Fracture Mechanics Equations

Timoshenko and Goodier(1951) present a solution for the deflection caused by a load distributed over the boundary of a semi-infinite elastic medium. We calculate fracture width from their solution, with the fracture plane perpendicular to the minimum reservoir stress direction, the load given by the difference between the fracture pressure and the minimum reservoir stress, a factor of two added because there are two fracture faces, and rock properties in the integrand since they can vary over the fracture face:

$$w(x,z) = 2\iint \frac{(1-\nu^2)}{\pi E r}(P - \sigma_{min}) r dr d\theta \tag{12}$$

where E is Young's modulus, ν is Poisson's ratio, P is fracture pressure, and σ_{min} is minimum reservoir stress. Barree and Conway (1994) have also used this approach to calculate fracture width.

Yew (1997) presents a fracture extension criterion. The stress intensity factor at the fracture tip is given by:

$$K_I = \frac{E}{8(1-\nu^2)}\sqrt{\frac{2\pi}{r}}w(r) \tag{13}$$

where r is the inward normal distance from the fracture front. The movement of the fracture front a distance d is given by

$$d = max\left\{ d_{max}\frac{K_I - K_{IC}}{K_{IC} + \frac{\sigma_{min} H_{frac}}{\sqrt{z_{loc}}}}, 0 \right\} \tag{14}$$

where K_{IC} is the rock critical stress intensity factor, H_{frac} is the local fracture height, and z_{loc} is the relative depth of the fracture.

3) Wellbore Formulation

A wellbore is coupled to the fracture in order to model the transit of slurry from the surface to the fractures. It consists of a series of connected linear well segments, with each having a starting and ending measured depth and true vertical depth, and constant outer and inner radii. Slurry segments flow through the well in a piston-like manner and the fluid components of slurry are assumed to be slightly compressible. Figure 1 shows a schematic of a wellbore. There are two well segments, a vertical one and a horizontal one, and three slurry segments.

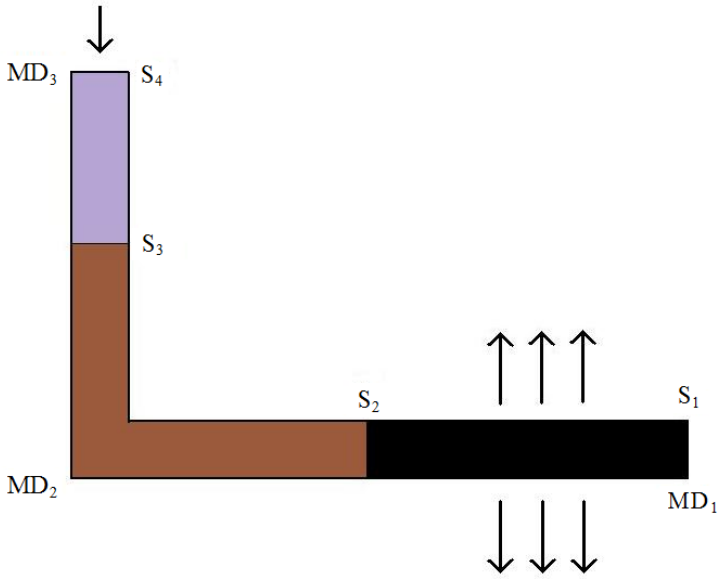

Figure 1.Schematic of wellbore with two segments and three stages. Single arrow denotes injection and arrow triplet denotes fluid loss to the surroundings. MD_i denotes measured depth and S_i denotes the slurry segment boundaries.

A mass balance for fluid and proppant for injected slurry segment is:

$$\frac{\partial}{\partial t}\int_{S_{i+1}}^{S_i} A\rho_x S_x dS + q_{loss}\rho_x S_x - q_{inj}\rho_x S_x = 0, x = f, p \tag{15}$$

where segment i is found from measured depth S_{i+1} to S_i along the wellbore, A is the well segment cross sectional area, q_{inj} is injection rate and the injection term is nonzero only for the slurry segment currently being injected, and q_{loss} is rate of fluid loss to the fracture for completed well segments.

The pressure gradient along the wellbore has frictional and gravitational components:

$$\frac{\partial P}{\partial s} = \rho \bar{g} \cdot \hat{s} + \frac{\partial P_{fric}}{\partial s} \tag{16}$$

where $\bar{g}$ is the gravitational vector, $\hat{s}$ is the unit vector in the direction of the wellbore, and P_{fric} is the frictional portion of the pressure gradient. This frictional portion is correlated with slurry Reynold's number.

4) Two-Phase Flow Model

The two phase flow model, consisting of gas and water (or liquid) in a porous or fractured unconventional reservoir, is similar to the two-phase black oil hydrocarbon model. For simplicity, the gas and water components are assumed to be present only in their associated phases and adsorbed gas is within the solid phase of rock. Each phase flows in response to pressure, gravitational, and capillary forces according to the multiphase extension of Darcy law or several extended non-Darcy flow laws, discussed below. In an isothermal system containing two mass components subject to multiphase flow and

adsorption, two mass-balance equations are needed to fully describe the system. For flow of phase β (g for gas and w for water):

$$\frac{\partial}{\partial t}(\phi S_\beta \rho_\beta + m_g) = -\nabla \bullet (\rho_\beta \mathbf{v}_\beta) + q_\beta \tag{17}$$

where ϕ is the effective porosity of porous or fractured media; S_β is the saturation of fluid β; ρ_β is the density of fluid β; v_β is the volumetric velocity vector of fluid β, determined by Darcy's law or non-Darcy flow models; t is time; m_g is the adsorption or desorption mass term for gas component per unit volume of rock formation; and q_β is the sink/source mass term of phase (component) β per unit volume of formation.

The Darcy velocity of phase β is defined as:

$$\vec{V}_\beta = -\frac{k k_{r\beta}}{\mu_\beta}\left(\nabla P_\beta - \rho_\beta g \nabla D\right) \tag{18}$$

The governing Equations (17) of mass conservation for the two phases need to be supplemented with constitutive equations, which express all the parameters as functions of a set of primary thermodynamic variables of interest. The following relationships will be used to complete the statement of describing multiple phase flow of gas and liquid through porous and fractured media (Wang et al., 2013, Wu et al., 2013).

- Saturation Constraint:

$$S_w + S_g = 1 \tag{19}$$

- Capillary Pressure Functions:

$$P_w = P_g - P_{cgw}\left(S_w\right) \tag{20}$$

where P_{cgw} is the gas-water capillary pressure in a two-phase system, which is assumed to be a function of water or gas saturation only.

- Relative Permeability Functions:

$$k_{rw} = k_{rw}\left(S_w\right) \tag{21}$$

$$k_{rg} = k_{rg}\left(S_g\right) \tag{22}$$

- PVT Data:

$$\rho_w = \frac{(\rho_w)_{STC}}{B_w} \tag{23}$$

$$\rho_g = \frac{Z_g M_g P}{RT} \tag{24}$$

where B_β is formation volume factor for phase β; $(\rho_\beta)_{stc}$ is density of phase β at standard condition (or storage tank conditions); M_g is average molecular weight; Z_g is the z factor to calibrate gas density from ideal gas to real gas; R is universal gas constant.

- Fluid Viscosities:

$$\mu_g = \mu_g\left(P_g\right) \tag{25}$$

- Formation Porosity:

$$\phi = \phi^{o}\left(1 + C_{r}\left(P - P^{o}\right) - C_{T}\left(T - T^{o}\right)\right) \tag{26}$$

where ϕ_0 is the effective porosity of formation at reference pressure of, P_0; and reference temperature, T_0; and C_T is thermal expansion coefficient of formation rock.

5) Flowchart for the Coupled Fracture and Flow Model

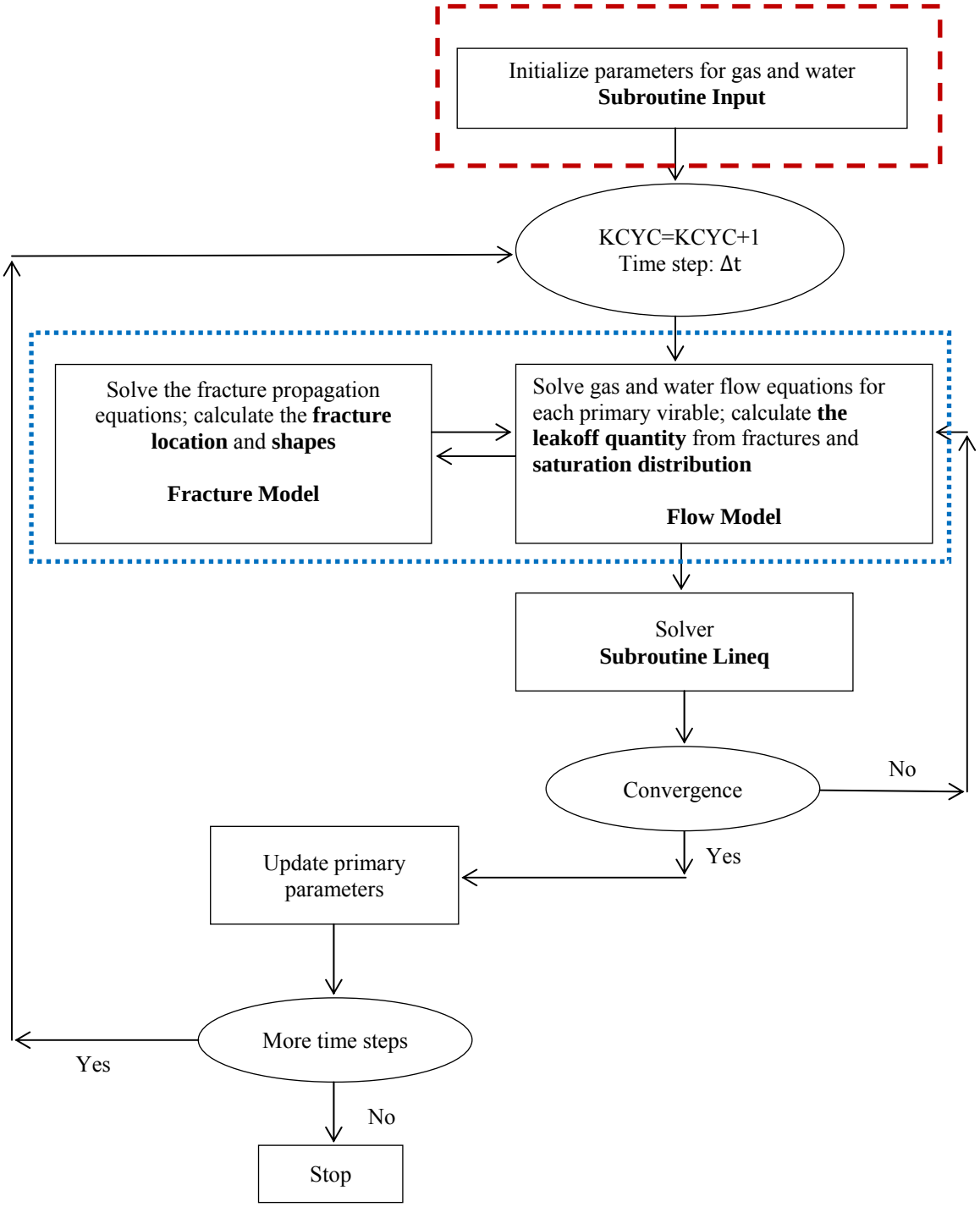

Figure 2. Flowchart of the Coupled Fracture and Flow Model

Example Simulation and Discussion

In our fracturing simulation, there are two slurry fluid components called BASEFL and GEL. Both are Newtonian fluids with reference density 1020 kg/m^3 and compressibility of $2 \cdot 10^{-10}$ Pa^{-1}. The viscosity of BASEFL is 0.001 Pa·s and the viscosity of GEL is 0.02 Pa·s. There is one proppant component with density 2800 kg/m^3 and diameter 0.00045 m.

The well consists of two segments. The first one is a vertical segment from the surface to 3253 m measured depth (Figure 3). The second segment is a horizontal one 1713 m long to 4966 m measured depth. The outer diameter of the first segment is 9.5 in (0.24 m), the outer of the second is 6 in (0.15 m), and the inner diameter of both is 2.25 in (0.06 m). There are two open-hole completions, the first one from 4510 to 4530 m and the second from measured depth 4270 to 4290 m.

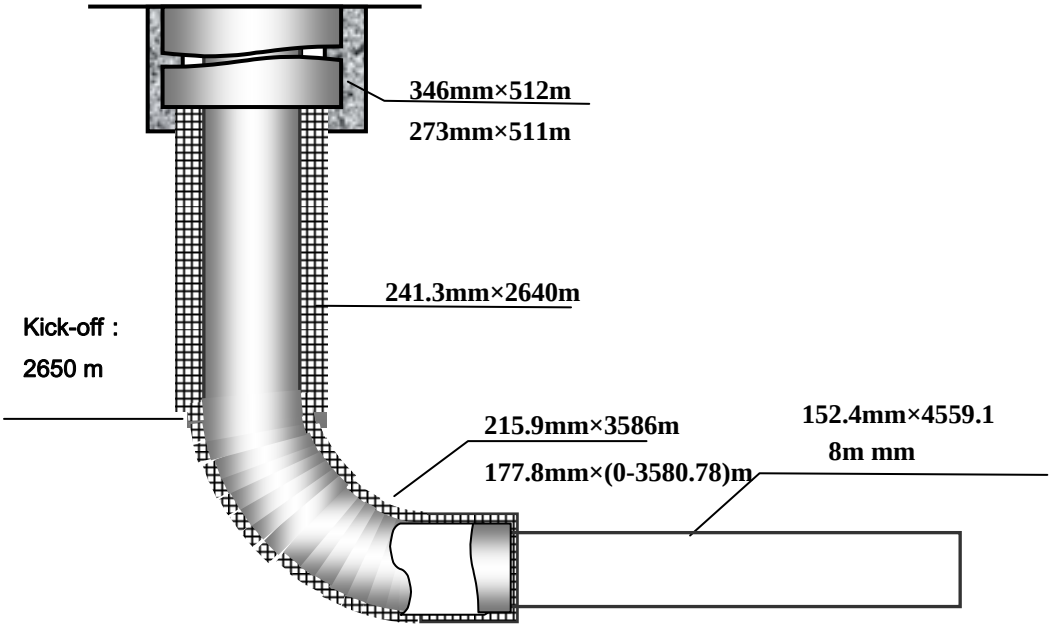

Figure 3 Well trajectory and structure data

An injected stage contains 15 slurry segments. Information about these 15 segments in a stage is shown in Table 1. The fracture gridblocks are square with length 10 m. Reservoir compressibility is 10^{-9} Pa^{-1} and reservoir viscosity is 0.0001 Pa·s. The maximum fracture front displacement parameter (d_{max} in Equation 14) is 1 m. The system is isothermal, the wellbore initially contained BASEFL with no proppant, and the horizontal wellbore is parallel to the normal vector to the minimum stress plane. Consequently, each completedinterval would have its own fracture. One slurry stage was injected into the first completed interval followed by another into the second completed interval with the first one.

Formation porosity is 0.772, permeability is 10^{-16} m^2, Young's modulus is 10 GPa, Poisson's ratio is 0.20, and tensile strength and toughness are both 5 MPa. Pressure is 10^{-1}MPa at the surface and 31.9 MPa at the completion true vertical depth. Maximum stress is 79 MPa at 2253 m true vertical depth and 90.3 MPa at 3253 m true vertical depth. Minimum stress is 65 MPa at 2253 m true vertical depth and 87.3 MPa at 3253 m true vertical depth.

Figures 4 shows the fracture width profile and Figure 5 shows the proppant volume fraction profile at the end of the second injected stage for the second completed interval. The dot indicates the intersection of the horizontal well with the fracture. Injected proppant has been swept away from the vicinity of the well by fluid-only segment 15 in Table 1. Areas of 0.6 proppant fraction, the maximum proppant fraction, occur mostly at the fracture bottom due to proppant settling and fluid leakoff.

Table 1.Injected slurry composition for a stage.

Segment	Volume, m3	Injection Rate, m3/sec	Proppant Volume Fraction	Fluid Component
1	13	0.0417	0.0	BASEFL
2	30	0.06	0.0	GEL
3	8.2	0.06	0.0244	GEL
4	15	0.06	0.0	GEL
5	8.3	0.06	0.0361	GEL
6	43.0	0.06	0.0	GEL
7	15.6	0.06	0.0385	GEL
8	17.2	0.06	0.0698	GEL
9	21.1	0.06	0.0995	GEL
10	23.6	0.06	0.1102	GEL
11	22.8	0.06	0.1228	GEL
12	18.5	0.06	0.1381	GEL
13	17.6	0.06	0.1477	GEL
14	7.1	0.06	0.1549	GEL
15	15.9	0.06	0.0	GEL

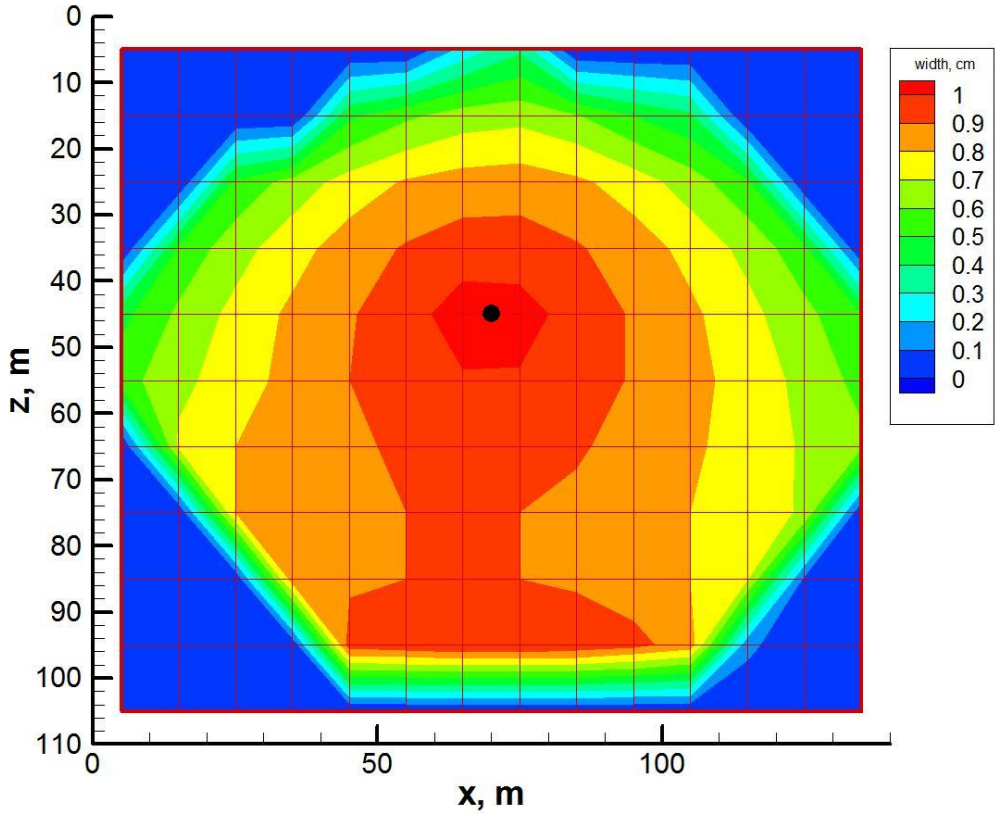

Figure 4. Fracture width profile at the end of the second stage for perforated interval 4270 to 4290 m.

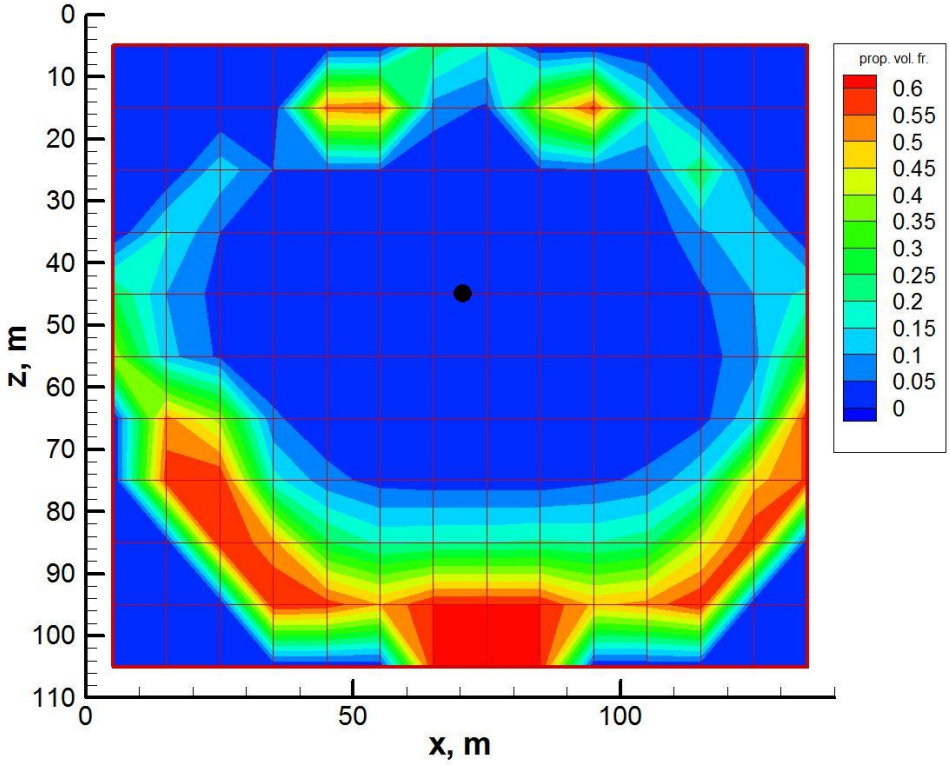

Figure 5. Proppant volume fraction profile at the end of the second stage for perforated interval 4270 to 4290 m.

For the two-phase flow model, wellbore pressure versus time is input, as shown in Figure 6, along with other data shown in Table 2 such as initial pressure, average porosity, gas saturation and so on. However, these data are not enough to specify the simulation and other parameters were estimated. Then, the calculated production rate is compared with the field data. They matched very well, indicating our simulation model can be applied to the analysis of field data, as shown inFigure 7.

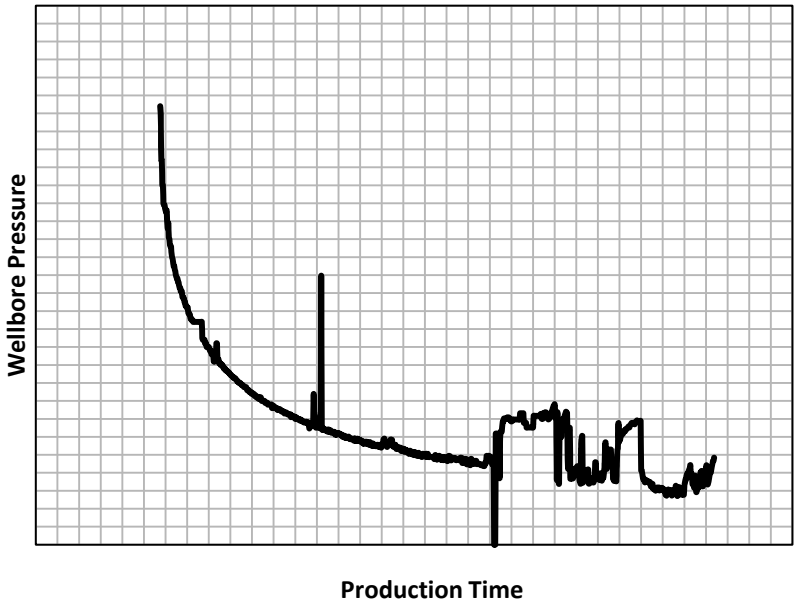

Figure 6. Wellbore pressure v.s. time as input data for history match

Table 2. Formation Evaluation Data

Parameters	Value	Units
Temperature, T	581.4	F
Effective permeability,	2.45	mD
Gas viscosity	1.84E-2	cp
Porosity,	0.05	
Gas compressibility,	2.80E-4	1/psi
Rock compressibility,	3.45E-6	1/psi

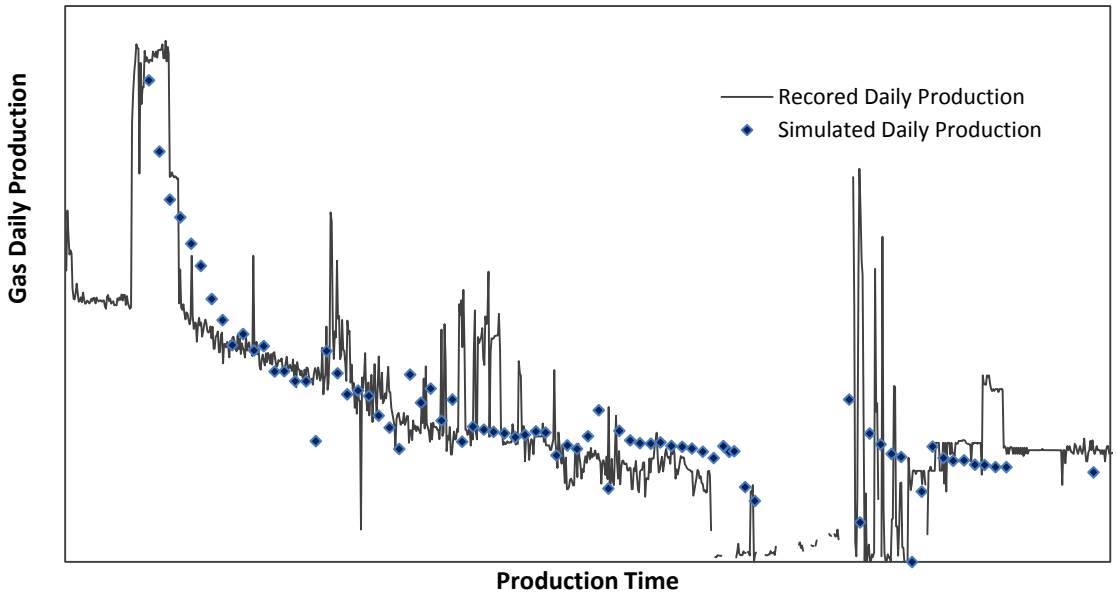

Figure 7. History-match of daily production data

Summary and Conclusions

We developed a coupled hydraulic fracturing propagation and gas well performance model for shale gas reservoirs. Several important processes are considered in this model including: fracture width increase and fracture propagation that occurs as slurry is injected into the fracture; erosion caused by fracturing fluid and leakoff; proppant subsidence and flowback; and multi-phase fluid flow through various-scaled anisotropic natural and man-made fractures. We showed the mathematical and physical equations for the model and the methodology used to couple the two parts. We conducted an example study using field data. We show the fracture propagation and well performance, and thesimulated results from this coupled model matched the production data very well.

Acknowledgement

This work was supported in part by EMG Research Center in Colorado School of Mines, CNPC-USA, and Fundation CMG. Permission by CNPC management to publish this work is gratefully acknowledged.

References

Barree, R. D. and Conway, M.: "Experimental and Numerical Modeling of Convective Proppant Transport," SPE 28564, presented at SPE 69th Annual Technical Conference and Exhibition, New Orleans, LA, September 25-28, 1994

Friehauf., K. E.: Simulation and design of energized hydraulic fractures, Ph.D. thesis,The University of Texas at Austin, 2009.

Nicodemo, L., Nicolais, L., and Landel, R.F.: Shear rate dependent viscosity suspensions in Newtonain and non-Newtonian liquids, Chemical Engineering Science, 29,729-735, 1974.

Timoshenko and Goodier: Theory of elasticity, McGraw-Hill Book Company, Inc, New York, NY 1951.

Wang, C., Ding, D., and Wu, Y.S., "Characterizing Hydraulic Fractures in Shale Gas Reservoirs Using Transient Pressure Tests", SPE-163819 presented at SPE Hydraulic Fracturing Technology Conference, the Woodlands, TX, USA, 2013

Wu, Y.S., Li, J., Ding, D., Wang, C., and Di, Y., "A Generalized Framework Model for Simulation of Gas Production in Unconventional Gas Reservoirs", SPE-163609 presented at the 2013 SPE Reservoir Simulation Symposium, the Woodlands, TX, USA, 2013

Yew, C. H.: Mechanics of hydraulic fracturing, Gulf Publishing Company, Houston, TX, 1997.